Novel Microfibrous-Structured Silver Catalyst for High Efficiency Gas-Phase Oxidation of Alcohols

Jiping Mao, Miaomiao Deng, Li Chen, Ye Liu, and Yong Lu
Shanghai Key Laboratory of Green Chemistry and Chemical Processes, Dept. of Chemistry, East China Normal University, Shanghai 200062, China

DOI 10.1002/aic.12088
Published online October 8, 2009 in Wiley InterScience (www.interscience.wiley.com).

Novel microfibrous-structured silver catalysts were developed for gas-phase selective oxidation of mono-/aromatic-/di-alcohols. Sinter-locked three-dimensional microfibrous networks consisting of 5 vol % 8-μm-Ni (or 12-μm-SS-316L) fibers and 95 vol % void volume were built up by the papermaking/sintering processes. Silver was then deposited onto the surface of the sinter-locked fibers by incipient wetness impregnation method. At relatively low temperatures (e.g., 380°C), the microfibrous-structured silver catalysts provided quite higher activity/selectivity compared to the electrolytic silver. The microfibrous Ag/Ni-fiber offered much better low-temperature activity than the Ag/SS-fiber. The interaction at Ag particles and Ni-fiber interface not only visibly increased the active/selective sites of Ag^{+} ions and $Ag_n^{\delta+}$ clusters but also significantly promoted their low-temperature reducibility and ability for O_2 activation. In addition, the microfibrous structure provided a unique combination of large void volume, entirely open structure, high thermal conductivity and high permeability. © 2009 American Institute of Chemical Engineers *AIChE J,* 56: 1545–1556, 2010

Keywords: silver catalysis, monolithic catalyst, microstructured reactor, fibers, alcohol, gas-phase oxidation

Introduction

Selective oxidation of alcohols to the corresponding carbonyl compounds is one of the most important chemical transformations in organic chemistry for both laboratory and industrial manufacturing. Carbonyl compounds such as aldehydes and ketones are the valuable synthetic intermediates for many drugs, vitamins, and fragrances.[1–3] Traditionally, such syntheses are mostly preformed in the presence of large amount of volatile organic solvents (e.g., ethanol, benzene, *p*-xylene, etc.) with stoichiometric inorganic oxidants, notably Cr reagents.[4–7] In nearly two decades, various catalytic systems using environmentally benign oxidants like molecular oxygen, hydrogen peroxide, organic peroxides under homogeneous (or heterogeneous) conditions have been developed,[3,5–13] aiming at replacing the traditional toxic and expensive stoichiometric oxidation processes. Among them, the gas-phase selective oxidation of alcohols shows great potential to develop efficient, cost-effective, and green processes for the production of carbonyl compounds.[8–13] It is desirable to significantly intensify the reaction heat removal from the catalyst bed, and meanwhile, to suppress the thermal cracking and over oxidation of the alcohols (especially the large molecules). A significant challenge facing this effort is the development of high-performance catalyst and/or new-type reactor with unique combination of excellent heat conductivity and high low-temperature activity/selectivity.

Some silver-based catalysts including electrolytic silver and supported silver catalysts, have been demonstrated recently for the selective oxidation of alcohols[8–13] in the

Correspondence concerning this article should be addressed to Y. Lu at ylu@chem.ecnu.edu.cn.

packed bed reactor. However, some serious problems still exist in the applications of such catalysts. For example, the electrolytic silver catalyst, widely used for methanol oxidation to produce formaldehyde using thin-bed reactor, has good thermal conductivity but is not active at below 500°C or not selective at above 500°C for the gas-phase oxidation of larger alcohols such as benzyl alcohol.[8,10] The supported silver catalysts using the carriers such as Al_2O_3, SiO_2, and SiC, have better catalytic activity at relatively low temperatures in the packed bed reactor.[9] However, their weak thermal conductivity easily generates partial hotspots in reaction beds for the strongly exothermic gas-phase selective oxidation of alcohols. This is not only a main cause of the catalyst degradation but also a hidden danger. More recently, the Au/SiO_2 catalysts with or without copper additives have been reported for the gas-phase selective oxidation of benzyl alcohol.[14] These Au-based catalysts delivered excellent low-temperature activity with very high target product selectivity. Nevertheless, bed-temperature increase of >40°C was observed even in a lab-scale microreactor owing to the poor thermal conductivity of the catalyst bed.[14] For the reasons given above, their practical applications are very limited.

Hence, it is important to render a new kind of catalyst and/or new-type reactor with not only good low-temperature activity/selectivity but also significantly intensified intrabed heat transfer. To accomplish this goal, a novel silver catalyst supported on LTA zeolite film[8] coated on a copper grid has been reported and demonstrates good low-temperature activity with high selectivity to benzaldehyde. Recently, a new class of microfibrous carriers using microfibers has been invented by Tatarchuk.[15,16] This approach has been extensively applied to develop high-efficiency miniature H_2 generator for fuel cell power supplies.[17–20] This microfibrous structure provides large void volume, entirely open structure, large surface-to-volume ratio, high permeability, high thermal conductivity and unique form factors. For applications that entrap small particles within or load active components (e.g., metals) on the microfibrous network, unique combinations of surface area, pore size/particle size, thermal conductivity, and large void volume are obtained. This approach permits high efficiency process and advanced design of reactor with many beneficial properties that avoid the frustrated problems encountered in the conventional approaches (e.g., conventional packed beds). Our previous microfibrous composites with entrapment of preferential oxidation (PROX) CO catalyst particulates and with entrapment of H_2S sorbent particulates for hydrogen fuel cleanup in proton exchange membrane fuel cell (PEMFC) applications do both provide a 3-fold or more promotion of bed utilization efficiency.[17–20] These approaches also lead to significant reduction of the overall reaction bed weight and volume compared to the packed beds with 1–2 mm dia. catalyst/sorbent pellets.[17–20] More interestingly, such microfibrous structure, with unique form factors, can be made into thin sheets (from submillimeter to several millimetres in thickness) of large area and/or pleated sheet structure to control pressure drop and contacting efficiency in a beneficial manner different from other traditionally employed contacting schemes including packed beds, fluid beds, honeycomb monoliths or wovens.[17,18]

Accordingly, it is safe to say that the microfibrous structure is an excellent and promising technology for the development of high-performance catalysts (or new-type microfibous bed reactor), especially for the strongly endothermic or exothermic reactions. Metal network structure definitely possesses the excellent thermal conductivity. For the strongly exothermic gas-phase oxidation of alcohols, the excellent heat conductivity of the catalytic bed facilitates the isothermal operation thereby likely ensuring the activity/selectivity maintenance. Nonporous structure of the microfibers results in the high accessibility of active components deposited on. Actually, the large void volume and the open structure as well as the excellent heat conductivity are the central notion in promoting the steady-state volumetric reaction rate.[21] Exactly, silver catalyst supported on a sinter-locked Ni-fiber has been reported and this novel microfibrous bed reactor indeed demonstrates good low-temperature activity for the gas-phase selective oxidation of benzyl alcohol with high target product selectivity.[10] However, the nature for their low-temperature activity as well as the reactivity of this new-type microstructured reactor for the other alcohols is still not clear.

In this study, sinter-locked three-dimensional microfibrous network consisting of 5 vol % 8 μm (dia.) Ni fibers or 12 μm (dia.) SS-316L fibers and 95 vol % void volume were utilized to support Ag by incipient wetness impregnation with $AgNO_3$. The reactivity of the microstructured catalytic bed incorporated with silver catalysts was measured in the case of gas-phase selective oxidation of mono-/di-alcohols and aromatic alcohols using O_2 as oxidants. The microfibrous Ag/Ni-fiber demonstrated much higher low-temperature activity/selectivity at 330–380°C and atmospheric pressure, compared to the packed bed with the electrolytic silver catalyst. To gain insight into the nature for the significant improvement of the low-temperature activity, the catalytically relevant physiochemical properties of the microfibrous-structured silver catalysts were studied by X-ray diffraction (XRD), O_2-chemisorption, H_2-temperature programmed reduction (H_2-TPR), O_2-temperature programmed oxidation (O_2-TPO), X-ray photoelectron spectroscopy (XPS), scanning electron microscope (SEM), and UV–visible diffuse reflectance spectroscopy (UV–vis DRS).

Experimental

Preparation of microfibrous-structured silver catalyst

The lab-scale thin-sheet microfibrous metal networks were built up by the wet-lay papermaking process[20] using 2–3 mm microfiber chops of Ni (8 μm diameter) and stainless steel 316L (SS-316L, 12 μm diameter), followed by the high-temperature sintering in hydrogen atmosphere. The detailed procedure for producing the microfibrous metal network is described as following: five grams of metal fibers and 1.7 g of cellulose fibers were added into water (1 L) and stirred vigorously to produce a uniform suspension. The resulting suspension was transferred into the head box of a 159 mm dia. circular sheet former (ZCX-159A, made in China) filled with 8 L water under manual mixing. A 159 mm circular preform was then formed by draining and drying in air. As-made preform paper was oxidized in air at

Table 1. Characteristics of the Typical Catalysts Studied

Catalyst	Ag/Ni-Fiber	Ag/Steel-Fiber	Electrolytic Silver*
Support	Ni-fiber	SS-fiber	–
Ag loading (wt %)	10.1	9.8	99.9
Void volume fraction (%)	95	95	43.5
Density (g cm^{-3})	0.33	0.33	3.5

*Particle size: 200–300 μm.

450°C to remove the cellulosic binders and subsequently sintered in hydrogen at 950°C for Ni fibers and at 1100°C for SS-316L fibers to create the three-dimensional sinter-locked networks. The resulting microfibrous networks were incipiently impregnated with the aqueous solution containing appointed amount of $AgNO_3$, dried overnight at 110°C and calcined in air at temperature range between 400 and 700°C for 4 h to obtain the microfibrous-structured silver catalysts. For comparison, electrolytic silver (supplied by the HePing noble metal catalyst company) was crushed and 200–300 μm particulates were collected for reaction use. Table 1 summarizes the characteristics of the typical catalysts studied.

Characterization

XRD patterns were obtained with a Bruker D8 ADVANCE diffractometer over a 2θ range of 20–85° in step of 0.02°, using Cu Kα radiation at an acceleration voltage of 40 kV. UV–vis DRS spectra were recorded in the range of 200–500 nm at room temperature using a Shimadzu UV-2400PC spectrophotometer. SEM images and Ag elemental mapping images of the catalysts were obtained on a Hitachi S4800 instrument equipped with an energy dispersive X-ray analyses (EDX) unit (Oxford, UK). XPS data were obtained on a Versaprobe Phi5000 ULVAC–PHI instrument using Al Kα radiation ($hv = 1486.6$ eV). The adventitious C1s line (binding energy of 284.6 eV) was used as reference for correcting charge shift.

The experiments on H_2-TPR, O_2-TPO, and O_2-chemisorption were carried out on a Quantachrome ChemBET 3000 chemisorption apparatus with a TCD. The sample loading was 0.1 g for each trial. The mixture of 5% H_2/Ar and mixture of 3% O_2/He were employed as carrier gases for both H_2-TPR and O_2-TPO tests, respectively. In these cases, the carrier gas flow rate was maintained at 40 mL/min while the temperature of sample was ramped at 10°C/min. Note that the samples after the H_2-TPR tests were cooled down to room temperature in a He flow and subsequently used for the O_2-TPO tests. O_2-chemisorption experiments were carried out at 200°C to determine the surface Ag atoms by assuming an O/Ag ratio of 1, according to Gavriilidis et al.[22] The samples were pre-reduced with 5% H_2/Ar at 300°C for 2 h and cooled down to 200°C in He flow. Subsequently, a sample of 3% O_2/He was pulsed, with a pulse volume of 100 μL, to the reactor every 5 min until the O_2 peak intensity remained unchanged.

Reactivity tests

The gas-phase selective oxidation of alcohols on these catalysts with molecular oxygen was carried out on a fixed-bed reactor under atmospheric pressure. The reactor was a quartz tube with an inner diameter (i.d.) of 16 mm. The catalysts were all loaded and directly exposed to the reactant stream without any pretreatment. The catalyst loading was 0.3 g for the microfibrous-structured silver catalysts but was 1.0 g for the electrolytic silver. For the microfibrous-structured silver catalysts, the circular chips (16.1 mm diameter) were punched down from their large sheet sample and packed layer-up-layer into the tube reactor. Note that the diameter of 0.1 mm larger than the i.d. of the tubular reactor was retained deliberately to avoid the appearance of the gap between the reactor wall and the edges of the catalyst chips thereby preventing the gas bypassing. Alcohols were fed continuously using a high-performance liquid pump, in parallel with O_2 (oxidant) and N_2 (diluted gas) feeding using the calibrated mass flow controllers, into the reactor heated to the desired reaction temperature. The reaction temperature, weight hourly space velocity (WHSV) and molar ratio of O_2 to alcoholic hydroxyl (O_2/ol) were varied in range from 300 to 500°C, 4 to 50 h^{-1}, and 0.4 to 1.0, respectively. The effluent was cooled using an ice-salt bath (−15°C) to liquefy the condensable vapors for analyzing by an HP 5890 gas chromatography-flame ionization detector (GC-FID) with a 60-m HP-5ms capillary column. The gas-phase products such as CO_2, CO and C1-C3 hydrocarbons were analyzed by an HP-5890 GC with thermal conductivity detector (TCD) and a 30-m AT-plot 300 capillary column.

Results and Discussion

Microfibrous structure and surface morphology

Figure 1 shows the microstructure, surface morphology and silver distribution of the microfibrous media. Figures 1a, d show the SEM images of the microfibrous structure and surface morphology of the sintered microfiber products before loading silver. Clearly, the sintering process led to a sinter-locked three-dimensional network while the large void volume and entirely open structure remained. Figures 1b, e show the surface morphology of the microfibrous structured Ag catalysts. The fiber surface became much rougher after loading Ag by impregnation method with the aqueous solution of silver nitrate. In comparison with the neat microfibers (Figures 1a, d), a number of particles appeared on the catalysts and the particle size was smaller for 10 wt % Ag/Ni-fiber (Figure 1b) than that for 10 wt % Ag/SS-fiber (Figure 1e). Figures 1c, f show the EDX element mapping images of Ag of the corresponding samples in Figures 1b, e, respectively. It is clearly that the Ag distribution by EDX was well consistent with the observation of the particles presented on the catalysts. This indicates that the particles as shown in Figures 1b, e were almost made up of Ag element and Ag was dispersed better on the Ni microfibers than on the SS-316L microfibers. Characteristic XRD peaks ascribed to Ag(111) (2θ: 38.1°), Ag(200) (2θ: 44.3°), Ag(220) (2θ: 64.4°), and Ag(311) (2θ: 77.5°) were clearly observed on the both microfibrous-structure supported silver catalyst samples,

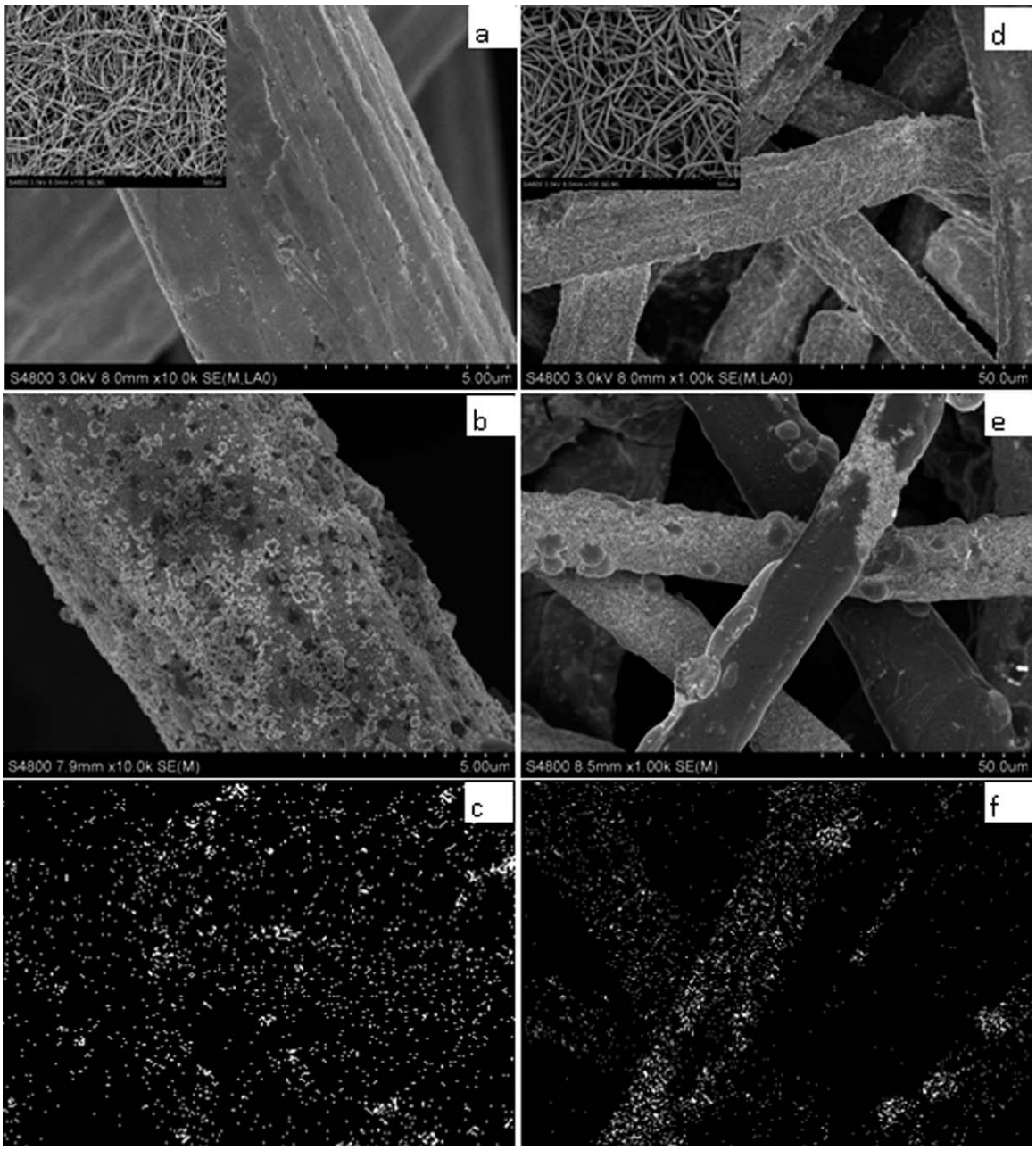

Figure 1. Morphology and microfibrous structure.

SEM images of sinter-locked 8-μm-Ni-fiber before (a) and after (b) loading 10 wt % Ag (10 wt % Ag/Ni-fiber), SEM images of sinter-locked 12-μm-SS-fiber before (d) and after (e) loading 10 wt % Ag (10 wt % Ag/SS-fiber). EDX Ag element mapping images of 10 wt % Ag/Ni-fiber (c) and 10 wt % Ag/SS-fiber (f).

indicating the silver in such two catalysts was mainly existed in the metallic state.

Catalytic performance

According to the different molecular structures or numbers of hydroxyl groups, alcohols can be divided into aromatic-alcohols, mono-alcohols and di-alcohols. Therefore, we selected benzyl alcohol, 1-butanol and 1,2-propylene glycol as the representatives of the different kind of alcohols for systematic tests in this study. Of course, extended tests for other alcohols including octanol, cyclohexanol, and phenethyl alcohol were also performed to examine the generality of our microfibrous-structured silver catalysts.

Gas-Phase Selective Oxidation of Aromatic and Alicyclic Alcohols: Effects of Ag Loading and Catalyst Calcination Temperature. Figure 2 shows the effects of Ag loading and catalyst calcination temperature on the performance of the Ag/Ni-fiber catalysts for gas-phase selective oxidation of benzyl alcohol at 380°C using a WHSV of 25 h^{-1}. As we can see, the reactivity of the Ag/Ni-fiber catalysts was greatly dependent on the Ag loading and catalyst calcination

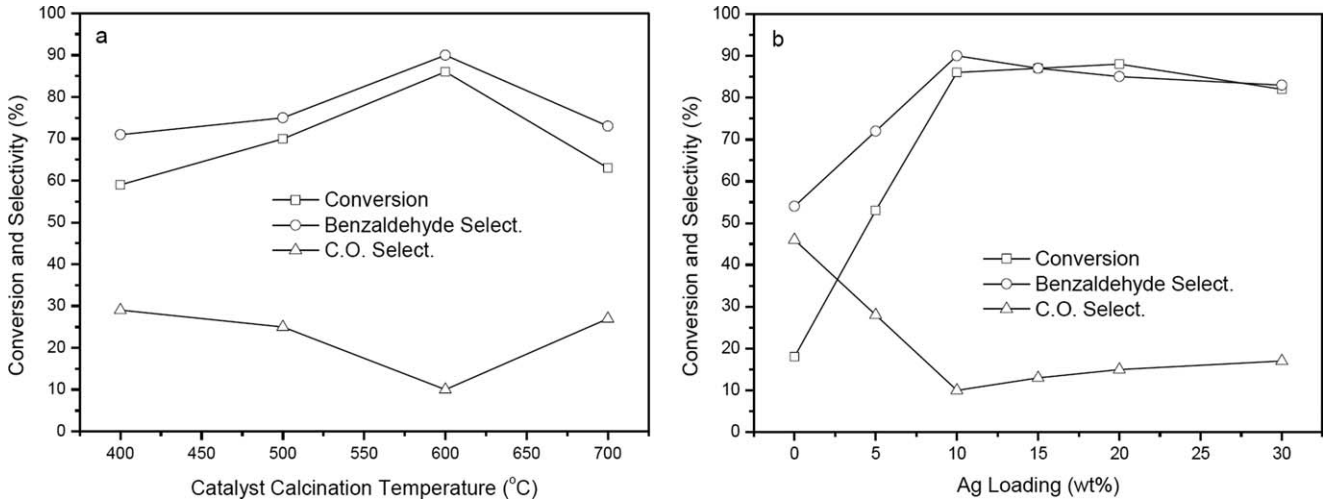

Figure 2. Effects of catalyst calcination temperature (a) and Ag loading (b) on the performance of Ag/Ni-fiber catalysts for gas-phase oxidation of benzyl alcohol at 380°C.

WHSV = 25 h^{-1}, molar ratio of O_2 to alcoholic hydroxyl (O_2/ol) = 0.6.

temperature under the compatible reaction conditions. For the Ag/Ni-fiber catalysts with Ag loading of 10 wt %, visible increase of benzyl alcohol conversion and selectivity to benzaldehyde was observed as the calcination temperature was increased from 400 to 600°C: 59% vs. 86% for conversion and 71% vs. 90% for selectivity to benzaldehyde (Figure 2a). As noted in previous work, Ag^+ ions and $Ag_n^{\delta+}$ clusters are active and selective for the gas-phase oxidation of alcohols.[8,23–26] Calcination at 600°C likely facilitated the formation of such active/selective sites on the surface of Ag/Ni-fiber catalysts thereby leading to good performance. Furthermore, some kind of new interaction between Ag and Ni-fiber at their interface was likely formed after calcination at 600°C. This was believed to further promote the activity/selectivity of the Ag/Ni-fiber catalysts since poor conversion (63%) and benzaldehyde selectivity (81%) were obtained when the sinter-locked SS-316L microfiber was used to replace the Ni-fiber carrier only. Further increase of the calcination temperature up to 700°C, however, significantly degraded both the conversion and selectivity of the Ag/Ni-fiber catalysts (Figure 2a), likely due to the severe sintering of Ag as well as the deep oxidation of the Ni-fiber. The

Table 2. Effects of Reaction Conditions on the Performance of Microfibrous-Structured Silver and Electrolytic Silver Catalysts for Gas-Phase Oxidation of Benzyl Alcohol*

Catalyst†	WHSV (h^{-1})	O_2/ol	Reaction Temp. (°C)	Conversion (%)	Selectivity (%) BzH‡	Selectivity (%) C.O.§	Yield (%) BzH‡
Ag/Ni-fiber¶	10	0.6	380	97	81	19	78
	20	0.6	380	92	86	14	79
	30	0.6	380	85	94	6	80
	40	0.6	380	76	92	8	70
	50	0.6	380	63	87	13	55
	20	0.4	380	79	90	10	63
	20	0.8	380	93	79	21	73
	20	1.0	380	95	73	27	69
	20	0.6	330	57	81	19	46
	20	0.6	350	73	82	18	60
	20	0.6	420	99	70	30	69
Ag/SS-fiber¶	10	0.6	450	92	84	16	77
	20	0.6	450	88	91	9	80
	30	0.6	450	85	90	10	76
	20	0.4	450	62	89	11	55
	20	0.8	450	91	79	21	72
	20	0.6	390	61	92	8	56
	20	0.6	480	90	71	29	64
Electrolytic silver	8	0.6	500	68	62	38	42
	20	0.6	500	55	79	21	43

*Each reaction condition was run for 3 h with mass balance of 93–96%, during which the experimental data were collected.
†The catalyst loading was 0.3 g for the microfibrous-structured silver catalysts but was 1.0 g for the electrolytic silver.
‡BzH = Benzaldehyde.
§C.O. = cracking and over oxidation byproducts.
¶Ag loading: 10 wt % (error: ±0.3 wt % by ICP (IRIS Intrepid II XSP)), calcination condition: 600°C in air for 4 h.

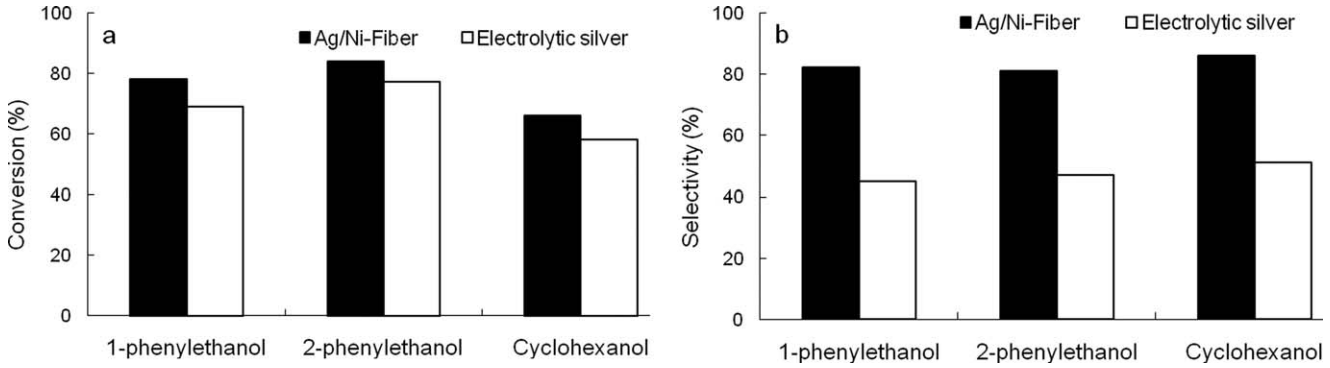

Figure 3. Comparison of conversion (a) and selectivity to carbonyl products (b) for gas-phase oxidation of various aromatic and alicyclic alcohols over 10 wt % Ag/Ni-fiber at 380°C and electrolytic silver at 500°C.

O_2/ol = 0.6, WHSV = 20 h^{-1}.

selectivity to byproducts (e.g., CO_2, benzene and toluene) showed a reverse tendency of the conversion and the benzaldehyde selectivity with the increase of the catalyst calcination temperature. For reference, the neat Ni-fiber carrier (i.e., Ag loading of 0 wt %) with pretreatment at 600°C in air was also tested and induced a conversion of 18% with a benzaldehyde selectivity of 54% only (Figure 2a).

To address the effect of Ag loading, the calcination temperature remained at 600°C for catalyst preparation. As shown in Figure 2b, Ag/Ni-fiber with the Ag loading of 10 wt % was the best catalyst for the selective oxidation of benzyl alcohol. In comparison with the neat Ni-fiber, the Ag loading of 5 wt % resulted in at once a significant increase of the conversion and selectivity. Increasing the Ag loading from 5 to 10 wt % greatly promoted the conversion and selectivity again. Further increasing the Ag loading to 20 wt % almost made no impact on the conversion but slightly degraded the selectivity to benzaldehyde. Further increasing the Ag loading up to 30 wt % visibly deteriorated both the conversion and selectivity.

Therefore, in the ongoing test experiments, the microfibrous structured silver catalysts with Ag loading of 10 wt % and catalyst calcination temperature of 600°C were employed if not specified.

Gas-Phase Selective Oxidation of Aromatic and Alicyclic Alcohols: Effects of Reaction Conditions. The effects of reaction conditions on the performance of Ag/Ni-fiber catalyst for the gas-phase selective oxidation of benzyl alcohol were carefully investigated, with the results as compiled in Table 2. It is clear that the optimal reaction temperature was 380°C with the WHSV of 30 h^{-1} and O_2/ol of 0.6; good conversion of 85% with the highest benzaldehyde selectivity

Table 3. Effects of Reaction Conditions on the Performance of Microfibrous-Structured Silver and Electrolytic Silver Catalysts for Gas-Phase Oxidation of *n*-Butanol*

Catalyst†	WHSV (h^{-1})	O_2/ol	Reaction Temp. (°C)	Conversion (%)	Selectivity (%)		Yield (%)
					B.A.‡	C.O.§	B.A.‡
Ag/Ni-fiber¶	10	0.6	380	77	80	20	62
	15	0.6	380	73	85	15	62
	20	0.6	380	68	89	11	60
	30	0.6	380	52	84	16	44
	40	0.6	380	46	79	21	36
	20	0.4	380	59	94	6	55
	20	0.8	380	61	82	18	50
	20	0.6	330	52	93	7	48
Ag/SS-fiber¶	10	0.6	450	78	79	21	62
	20	0.6	450	71	87	13	62
	30	0.6	450	63	83	17	52
	40	0.6	450	57	78	22	44
	20	0.4	450	51	64	36	33
	20	0.8	450	80	80	20	64
	20	0.6	390	61	79	21	48
	20	0.6	480	74	82	18	61
Electrolytic silver	8	0.6	500	61	32	68	20
	20	0.6	500	43	60	40	26

See footnote "" in Table 2.
†See footnote "†" in Table 2.
‡B.A. = *n*-butylaldehyde.
§See footnote "§" in Table 2.
¶See footnote "¶" in Table 2.

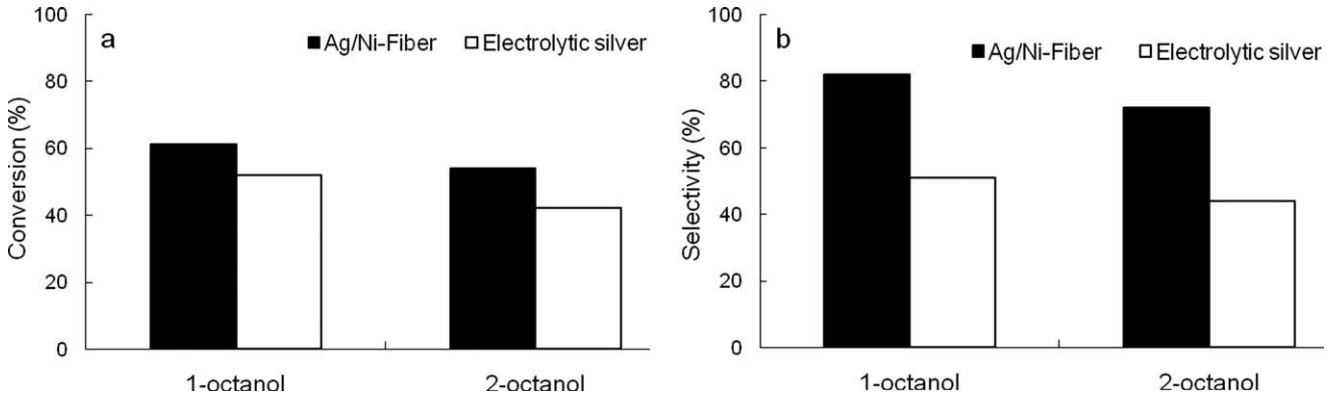

Figure 4. Comparison of conversion (a) and selectivity to carbonyl products (b) for gas-phase oxidation of various acyclic alcohols over 10 wt % Ag/Ni-fiber at 380°C and electrolytic silver at 500°C.

O_2/ol = 0.6, WHSV = 20 h^{-1}.

of 94% was obtained, corresponding to the best target product yield of 80%. When the reaction temperature was increased from 330 to 420°C using WHSV of 20 h^{-1} and O_2/ol of 0.6, the conversion of benzyl alcohol was increased from 57% to 99% but the best selectivity of 86% was presented at 380°C. At 380°C and WHSV of 20 h^{-1}, increasing O_2/ol from 0.4 to 0.6 obviously promoted the conversion but degraded the target product selectivity a little; further increasing the O_2/ol from 0.6 to 1.0 provided a little increase in conversion but obviously deteriorated the selectivity to benzaldehyde. At 380°C and O_2/ol of 0.6, conversion of benzyl alcohol was smoothly decreased from 97% to 63% with the increase of WHSV from 10 to 50 h^{-1}, but the selectivity to benzaldehyde reached maximum (94%) at the WHSV of 30 h^{-1} and almost was retained at this point with further increasing the WHSV up to 50 h^{-1}.

Gas-Phase Selective Oxidation of Aromatic and Alicyclic Alcohols: Comparison. Test experiments on the gas-phase selective oxidation of benzyl alcohol on the Ag/SS-fiber and electrolytic silver catalysts were performed for comparison. The reaction results are also shown in Table 2. Clearly, the 10 wt % Ag/Ni-fiber catalysts delivered much higher conversion and selectivity compared to the electrolytic silver catalysts, even operating the reaction at much lower reaction temperature (380°C vs. 500°C) with quite higher WHSV (30 h^{-1} vs. 8 h^{-1}). The 10 wt % Ag/SS-fiber did not yet yield better low-temperature activity/selectivity than the 10 wt % Ag/Ni-fiber throughout the entire reaction parameter range studied here. Note that the target product yield of 80% was also achievable at 450°C.

It was estimated that the Ag/Ni-fiber catalysts provided at least 4-fold promotion of the catalytic bed utilization efficiency (i.e., much higher WHSV: 40 h^{-1} vs. 8 h^{-1}) compared to the electrolytic silver, on the base of the equivalent alcohol conversions: 76% for Ag/Ni-fiber at 380°C; 68% for electrolytic silver at 500°C. Moreover, this new approach permitted dramatic saving of Ag: the microfibrous bed of 10 wt % Ag/Ni-fiber catalyst (0.3 g) has only 0.03 g Ag, only 3% that of the electrolytic silver (1.0 g in present work).

Test experiments on the gas-phase oxidation of phenethyl alcohol and cyclohexanol for both the 10 wt % Ag/Ni-fiber and electrolytic silver catalysts were also performed with the results as shown in Figure 3. Our 10 wt % Ag/Ni-fiber catalyst exhibited much higher conversion and selectivity to the corresponding target products even at quite low temperature with very high WHSV, compared to the electrolytic silver catalyst. Clearly, this microfibrous structured catalyst demonstrated highly effective and efficient gas-phase oxidation of aromatic and alicyclic alcohols, with significantly promoted low-temperature reactivity and multifold amplification of the reactor throughput.

Gas-Phase Selective Oxidation of Acyclic Mono-Alcohols. Table 3 shows the conversion and product selectivity for the gas-phase selective oxidation of *n*-butanol, using the 10 wt % Ag/Ni-fiber, 10 wt % Ag/SS-fiber and electrolytic silver catalysts. As in the case of benzyl alcohol, the conversion and product selectivity were dependent on the catalysts and significantly affected by the WHSV, O_2/ol and reaction temperature. The Ag/Ni-fiber and Ag/SS-fiber catalysts were more active and selective in the gas-phase oxidation of *n*-butanol to *n*-butylaldehyde under relatively mild reaction conditions, compared to the electrolytic silver catalyst. Likewise, the 10 wt % Ag/SS-fiber catalyst had not yield the activity/selectivity better than that for the 10 wt % Ag/Ni-fiber yet, being further confirmed the existence of special Ag-Ni interaction that is contributed to the good low-temperature activity/selectivity. In addition, with the increase of WHSV, O_2/ol and reaction temperature, the conversion and selectivity evolution for the selective oxidation of butanol was alike with that for the selective oxidation of benzyl alcohol. We also proceeded to investigate the effects of Ag loading and catalyst calcination temperature on the performance of Ag/Ni-fiber catalyst for the selective oxidation of *n*-butanol, indicating that the 10 wt % Ag/Ni-fiber calcined at 600°C still was the best catalyst.

Figure 4 shows the conversion and target product selectivity for the selective oxidation of 1-octanol and 2-octanol using 10 wt % Ag/Ni-fiber and electrolytic silver catalysts. Clearly, the traditional electrolytic silver catalyst had not yielded better activity for all alcohols than our microfibrous catalyst yet, even operating at 500°C. In addition, operation at elevated temperature facilitated the thermal cracking and over oxidation processes thereby leading to poor selectivity for the electrolytic silver catalyst. In contrast, the good low-

Table 4. Effects of Reaction Conditions on the Performance of Microfibrous-Structured Silver and Electrolytic Silver Catalysts for Gas-Phase Oxidation of 1,2-Propylene Glycol*

Catalyst†	WHSV (h^{-1})	O_2/ol	Reaction Temp. (°C)	Conversion (%)	Selectivity (%)			Yield (%)
					H.P.‡	M.G.§	C.O.¶	M.G.§
Ag/Ni-fiber**	15	0.6	330	93	22	70	8	65
	15	0.7	330	96	17	72	11	69
	15	0.8	330	99	8	83	9	82
	15	0.9	330	99	7	67	26	66
	15	0.6	300	63	28	58	14	36
	15	0.6	360	96	23	48	29	46
	8	0.6	330	97	18	58	24	56
	25	0.6	330	87	27	64	9	56
Ag/SS-fiber**	15	0.6	380	97	33	50	17	48
	15	0.7	380	98	24	55	21	54
	15	0.8	380	98	20	47	33	46
	15	0.7	360	91	27	46	27	42
	15	0.7	400	99	18	36	46	36
	8	0.7	380	99	19	46	35	45
	25	0.7	380	89	28	53	19	47
Electrolytic silver	4	0.8	450	97	23	37	40	36
	8	0.8	450	90	29	42	29	38

See footnote "" in Table 2.
**Ag loading: 20 wt % [error: ±0.3 wt % by ICP (IRIS Intrepid II XSP)], calcination condition: 600°C in air for 4 h.
†See footnote "†" in Table 2.
‡H.P. = 1-hydroxy-2-propanone.
§M.G. = methyl glyoxal.
¶See footnote "¶" in Table 2.

temperature activity of the Ag/Ni-fiber catalyst ensured the high conversion while effectively suppressing the thermal cracking and over oxidized products generated at elevated temperatures, and therefore, a higher yield of the target aldehydes could be easily obtained. Moreover, multifold increase of the WHSV resulted in a high yielding rate of the target aldehydes.

Gas-Phase Selective Oxidation of 1,2-Propylene Glycol. In comparison with the aforementioned mono-/aromatic-alcohols, the selective oxidation of di-alcohols is particularly challenging due to the one more hydroxyl group. Take for instance the selective oxidation of 1,2-propylene glycol of which the target product is methyl glyoxal. However, lean-oxidation to form hydroxyketone is likely superior to the moderate oxidation. Because of the existence of the secondary hydroxyl group, the 10 wt % Ag/Ni-fiber catalyst calcined at 600°C is the best one for the mono-/aromatic-alcohols but likely not for the 1,2-propylene glycol. Therefore, the effects of Ag loading and catalyst calcination temperature on the performance of Ag/Ni-fiber catalyst for this reaction were investigated firstly. It was found that the optimal catalyst calcination temperature was still 600°C but the best Ag loading was changed to 20 wt %.

Table 4 shows the conversion and product selectivity for the selective oxidation of 1,2-propylene glycol catalyzed by the 20 wt % Ag/Ni-fiber and the electrolytic silver catalysts. Our microfibrous catalyst provided excellent low-temperature activity with quite high selectivity to methyl glyoxal compared to the electrolytic silver catalyst. At a conversion of 97–99%, the 20 wt % Ag/Ni-fiber delivered the best target product selectivity [83%, two times as high as that (37%) of the electrolytic silver] while leading to a decrease in the reaction temperature by 120°C and a onefold increase of WHSV. In addition, the 10 wt % Ag/Ni-fiber catalyst delivered a conversion of only ~20% at 330°C using a O_2/ol of 0.8 and WHSV of 8 h^{-1}, about one fifth that of the 20 wt % Ag/Ni-fiber catalyst. The reason for this is not clear yet.

O_2 chemisorption: silver dispersion

It is widely accepted that highly dispersed metal particles show high catalytic activity due to a high fraction of surface metal atoms. We asked ourselves if the Ag dispersion of these catalysts was different thereby leading to the difference in their reactivity evolution. To make clarity, Ag dispersion of the catalyst samples was determined using O_2 chemisorption at 200°C with results as summarized in Table 5. According to Gavriilidis et al.,[22] the supported silver catalysts can reach the mono-layer saturated chemisorption of O atom at 200°C. As shown in Table 5, the supported Ag catalyst samples delivered equivalent surface Ag atoms; the electrolytic silver had surface Ag atoms two times as high as the supported silver catalysts.

For comparison, the turnover frequencies (TOFs) to benzyl alcohol were calculated by normalizing the benzyl alcohol conversion by the number of surface Ag atoms per gram catalyst. At equivalent benzyl alcohol conversion (60–70%) at O_2/ol of 0.6, the TOFs were: 57 s^{-1} for 10 wt % Ag/Ni-fiber under 380°C and WHSV of 50 h^{-1}, 26 s^{-1} for 10 wt % Ag/

Table 5. Results of O_2-Chemisorption at 200°C

Catalyst	Ag/Ni-Fiber*	Ag/SS-fiber*	Electrolytic Silver
O_2 in-take ($\mu mol/g_{cat.}$)	1.25	1.08	2.22
Surface Ag atoms per gram catalyst ($\times 10^{18}$)	1.38	1.20	2.45

*Ag loading: 10 wt %, calcination condition: 600°C in air for 4 h.

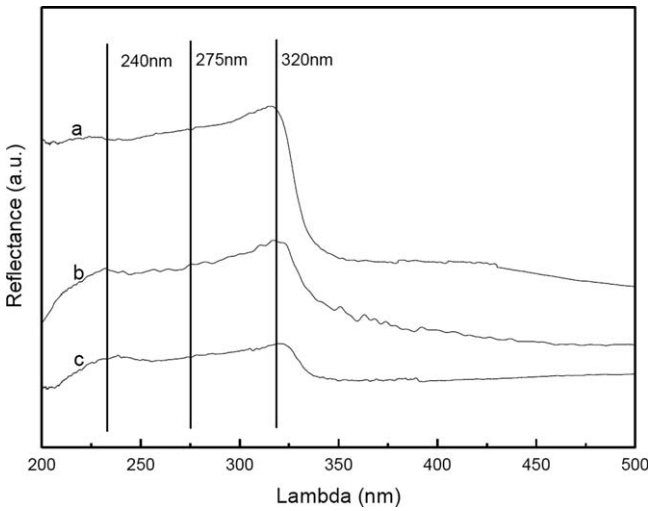

Figure 5. UV–vis DRS spectra of electrolytic silver (a), after calcination at 600°C in air for 2 h, 10 wt % Ag/Ni-fiber (b), and 10 wt % Ag/SS-fiber (c).

SS-fiber under 450°C and WHSV of 20 h^{-1}, and 13 s^{-1} for electrolytic silver under 500°C and WHSV of 10 h^{-1}. Clearly, no correlation between activity of the catalysts and their surface Ag atoms could be established, likely suggesting that the difference in the electronic properties of the catalyst samples might be the main cause for their quite different catalytic performance.

UV–vis DRS and XPS: Active sites

As generally accepted, Ag^+ ions and $Ag_n^{\delta+}$ clusters are active and selective for the gas-phase oxidation of alcohol.[8,23–26] Is it possible that the catalyst samples had quite difference in the active site (Ag^+ ions and $Ag_n^{\delta+}$ clusters) concentration thereby leading to the different catalytic activity? To answer this question, the chemical state of silver particles in the silver-based catalysts was analyzed using UV–vis DRS technique. Figure 5 shows the UV–vis DRS spectra of 10 wt % Ag/Ni-fiber, 10 wt % Ag/SS-fiber and electrolytic silver catalysts. As noted in previous work,[27–30] the metallic silver particles provide the UV–vis absorption band in the region of 310–320 nm; the isolated Ag^+ ions and charged $Ag_n^{\delta+}$ clusters deliver those in region of 230–250 nm and 270–290 nm, respectively. As shown in Figure 5, a strong sharp peak at about 320 nm, a weak peak at ~230 nm and a faint peak at ~275 nm, appeared on the electrolytic silver catalyst, indicating the existence of a large amount of metallic silver film or large particles with a relatively low concentration of isolated Ag^+ ions and charged $Ag_n^{\delta+}$ clusters. In contrast, on the 10 wt % Ag/Ni-fiber and 10 wt % Ag/SS-fiber catalysts, the peak at 320 nm weakened dramatically while the other two peaks especially the one at ~240 nm became strong. This indicates that the 10 wt % Ag/Ni-fiber and 10 wt % Ag/SS-fiber catalysts had higher concentration of isolated Ag^+ ions and/or $Ag_n^{\delta+}$ clusters than the electrolytic silver catalyst. Not surprisingly, our novel 10 wt % Ag/Ni-fiber and 10 wt % Ag/SS-fiber catalysts provided much higher catalytic activity for the gas-phase selective oxidation of alcohols than the electrolytic silver (Tables 2–4, Figures 2–4).

Whereas Ag/Ni-fiber and Ag/SS-fiber catalysts had very similar UV–vis spectra (Figure 5), it seems not safe to say that both of them had equivalent concentration of Ag^+ ions and $Ag_n^{\delta+}$ clusters. So, XPS measurements for these two catalysts were performed to quantitatively determine the surface concentration of Ag with different chemical states. Nevertheless, it is difficult to identify the chemical state of Ag element from the binding energy (BE) of Ag, because the BE difference between metallic Ag and oxidized Ag is very small and the BE assignment of Ag element remains controversial.[8,31,32] Therefore, the O1s spectra were recorded on the surfaces of the Ag/Ni-fiber and Ag/SS-fiber catalysts as shown in Figure 6. On the surface of Ag/Ni-fiber catalyst, the O existed in four forms with the BE of 529.3, 529.8, 530.6, and 531.5 eV (Figure 6a). The O1s peaks at 529.3 and 530.6 eV were assignable to the strongly chemisorbed O (O_γ) and subsurface O (O_β),[26] which were corresponding to

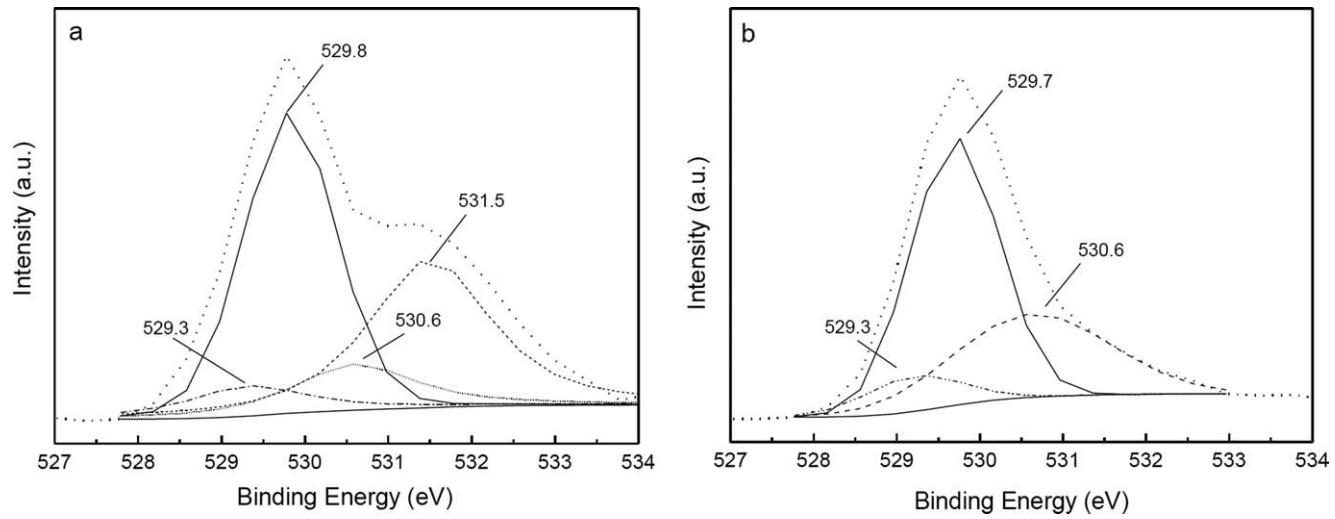

Figure 6. XPS O1*s* spectra of the 10 wt % Ag/Ni-fiber (a) and 10 wt % Ag/SS-fiber (b).

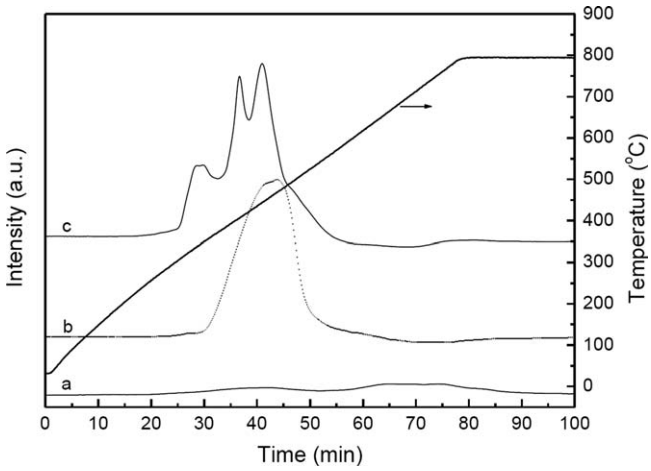

Figure 7. H_2-TPR profiles of electrolytic silver (a, after calcination in air for 2 h), Ni-fiber (b, calcined at 600°C in air for 4 h), and 10 wt % Ag/Ni-fiber (c).

the Ag^+ ions and $Ag_n^{\delta+}$ clusters; the peaks of O1s at 529.8 and 531.5 eV were associated to the lattice O atoms of NiO and Ni_2O_3, respectively.[32,33] Similarly, on the surface of Ag/SS-fiber, three O1s peaks with BE of 529.3, 529.7, and 530.6 eV were observed (Figure 6b), being ascribable to the strongly chemisorbed O (O_γ) and the lattice O atoms of Fe_2O_3 and Cr_2O_3, respectively.[34–36] For the Ag/SS-fiber sample, the assignment of the O1s peak with BE of 530.6 eV to Cr_2O_3 was strongly confirmed by the facts that the atom ratio of such O to Cr was very close to 1.5 and no clear H_2-reduction peak of O_β species could be detected by H_2-TPR analysis (see posterior section). Moreover, the surface Ag fraction in the total surface metal atoms were determined by XPS to be 25% (i.e., Ag/Ni = 1/3 for 10 wt % Ag/Ni-fiber; Ag/Fe/Cr = 1/2/1 for 10 wt % Ag/SS-fiber), being well consistent with the O_2-chemisorption results (see Table 5). For comparison, the amount of the surface O atoms with the BE of 529.3 eV was normalized by the amount of the surface Ag atoms to indicate the concentration of the Ag^+ ions and $Ag_n^{\delta+}$ clusters in the microfibrous-structure supported silver catalyst samples. Such value number was 0.08 for the 10 wt % Ag/SS-fiber, about a half that (0.14) for the 10 wt % Ag/Ni-fiber. It seems correlated well with the observation that the latter catalyst always provided higher activity than the former one under compatible conditions (see Tables 2–4). However, it is not clear yet why the Ag/Ni-fiber delivered much better low-temperature activity/selectivity than the Ag/SS-fiber. For instance, the Ag/Ni-fiber provided a reduction of the reaction temperature by 50–70°C and delivered compatible conversion with equivalent or higher target product selectivity for the gas-phase selective oxidation of alcohols, in comparison with the Ag/SS-fiber.

H_2-TPR and O_2-TPO: Catalyst reducibility and ability for O_2 activation

Experiments on the H_2-TPR for the microfibrous-structure supported silver catalysts and electrolytic silver were performed to study their discrepancy in the reducibility with the results as shown in Figure 7. For reference, the microfibrous-structured Ni-fibers and SS-fibers, which experienced 4-h calcination in air at 600°C, were also studied by H_2-TPR and their profiles were collected in Figure 7. Clearly, the silver catalyst samples studied here presented quite different reduction features. Figure 7a shows the H_2-TPR profile for the electrolytic silver recorded after exposure to O_2 for 2 h at 600°C. Two overlapped peaks appeared on the profile with the maximum at 450°C and 530°C, likely being contributed to the Ag species with subsurface oxygen (O_β) and strongly chemisorbed oxygen (O_γ).[26] Nevertheless, the reduction peak for the Ag species with weakly chemisorbed oxygen (O_α) was not observed clearly. It has been reported that volume diffusion of oxygen into silver is facilitated at elevated temperature thereby leading to the disappearance of O_α.[26] The calcined Ni-fiber sample gave a single-peak profile with the maximum at 450°C, being ascribable to the NiO (Figure 7b). The 10 wt % Ag/Ni-fiber catalyst offered a profile mainly consisting of an intense peak with a maximum at 430°C, a strong sharp peak at 400°C, a weak broad peak at 330°C and a visible shoulder peak at 500°C (Figure 7c). According to Figure 7b and the fact that large amount of surface O for NiO and small amount of surface O for Ni_2O_3 were detected by XPS on the 10 wt % Ag/Ni-fiber, the intense peak at 430°C and the shoulder peak at 500°C in the profile of Figure 7c were likely assignable to the NiO and Ni_2O_3, respectively. Therefore, the peaks at 400°C and 330°C were both contributed to the reduction of Ag species with O_γ and O_β. Actually, both O_γ (O1s: 529.3 eV) and O_β (O1s: 530.6 eV) species were detected by XPS (Figure 6a). Moreover, the H_2 consumption amount from the reduction of Ag species with O_γ and O_β was much larger for the 10 wt % Ag/Ni-fiber sample than those for the electrolytic silver (Figure 7). By comparison, it is safe to say that the 10 wt % Ag/Ni-fiber catalyst had much larger amount of Ag^+ ions and $Ag_n^{\delta+}$ clusters and such Ag sites were more active (corresponding to good low-temperature reducibility), in comparison with the electrolytic silver.

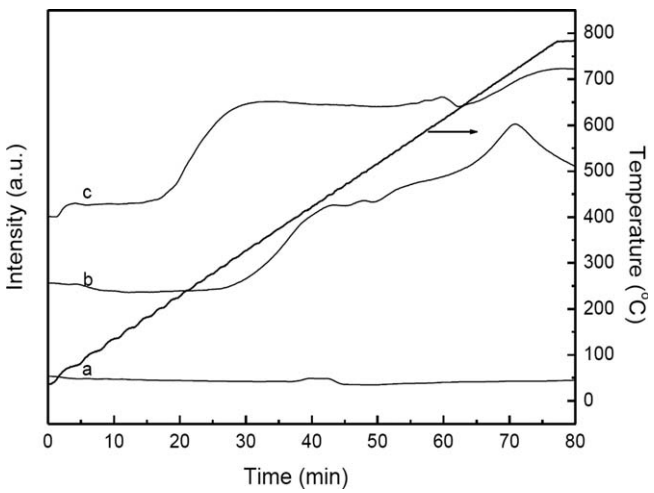

Figure 8. O_2-TPO profiles of electrolytic silver (a), Ni-fiber (b), and 10 wt % Ag/Ni-fiber (c).

Note: the samples are the corresponding ones after H_2-TPR experiments in Figure 7.

In addition, the 10 wt % Ag/SS-fiber and the SS-316L fiber pre-calcined in air at 600°C for 4 h were also studied by H_2-TPR. Unfortunately, their profiles were complex and similar, having the dominant peaks above 500°C. By comparison, only a very weak and broad new peak at 480°C was gleamingly presented for the 10 wt % Ag/SS-fiber, likely being assignable to the Ag species with O_γ since such O species were clearly observed on the O1s XPS spectrum for the 10 wt % Ag/SS-fiber (Figure 6b). Especially, no clear Ag^+ and $Ag_n^{\delta+}$ reduction peaks compatible to those for the 10 wt % Ag/Ni-fiber could be found out below 450°C on the 10 wt % Ag/SS-fiber. The above results suggest that the 10 wt % Ag/SS-316L catalyst had lower concentration of Ag^+ and $Ag_n^{\delta+}$ and such Ag sites were not so active (required higher temperature for H_2-reduction) as those on 10 wt % Ag/Ni-fiber. Therefore, like the electrolytic silver, this catalyst showed high activity only at higher temperatures (e.g., 450°C for the gas-phase selective oxidation of benzyl alcohol).

Experiments on the O_2-TPO for the samples after the H_2-TPR tests were also performed for comparative study of their ability to activate O_2, with the results as shown in Figure 8. Figure 8a shows the O_2-TPO profile for the electrolytic silver, giving a very weak O_2 consumption peak with maximum at 420°C. Ni-fiber sample provided a profile containing multioverlapped peaks for the oxidation of Ni with the first one centered at ~420°C (Figure 8b). A profile containing multioverlapped peaks was also obtained for the 10 wt % Ag/Ni-fiber, but a new strong peak appeared with the maximum at 320°C (Figure 8c) compared with the profile of Ni-fiber sample (Figure 8b). This is likely assignable to the oxidation of the reduced Ag active sites. Such low oxidation temperature indicates that this microfibrous catalyst was much more active for O_2 activation than the electrolytic silver. In addition, O_2 consumption amount concerning the oxidation of reduced Ag sites was much larger for the 10 wt % Ag/Ni-fiber than that for the electrolytic silver. This confirms again that the 10 wt % Ag/Ni-fiber catalyst had much higher concentration of the active Ag sites, being consistent with the information provided by the H_2-TPR experiments and XPS analyses.

Accordingly, the Ag/Ni-fiber catalyst not only provided high concentration of Ag^+ ions and $Ag_n^{\delta+}$ clusters but also exhibited significantly enhanced low-temperature reducibility and the ability for low-temperature activation of O_2. It is reasonable to explain why the Ag/Ni-fiber catalyst exhibited much better low-temperature activity than the Ag/SS-316L and electrolytic silver catalysts.

Conclusion

A promising thin-sheet microfibrous structured silver catalyst system for the gas-phase selective oxidation of various alcohols was developed by placing Ag onto the surface of the sinter-locked three-dimensional networks consisting of 5 vol % 8-μm-Ni- and 12-μm-(SS-316L)-fibers through the incipient wetness impregnation method. The best microfibrous structured silver catalyst was the Ag/Ni-fiber that was calcined at 600°C in air and had Ag-loading of 10 wt % for mono-alcohols or 20 wt % for di-alcohols. In comparison with the Ag/SS-fiber and electrolytic silver, the Ag/Ni-fiber catalyst not only provided high concentration of Ag^+ ions and $Ag_n^{\delta+}$ clusters but also exhibited significantly enhanced low-temperature reducibility and the ability for low-temperature activation of O_2 molecules. As a result, such catalyst demonstrated pleasing low-temperature activity/selectivity for the gas-phase selective oxidation of alcohols. For instance, the conversion and product selectivity results on the Ag/Ni-fiber against the electrolytic silver were: 99% and 83% at 330°C vs. 90% and 42% at 450°C in the gas-phase selective oxidation of 1,2-propylene glycol to methyl glyoxal; 92% and 86% at 380°C vs. 55% and 79% at 500°C in the gas-phase selective oxidation of benzyl alcohol to benzaldehyde. In addition, the microfibrous Ag/Ni-fiber catalyst provided a significant (fourfold or more) promotion of the steady-state volumetric reaction rate compared to the electrolytic silver.

Acknowledgments

Y. Lu gratefully thanks the Program for New Century Excellent Talents in University (NCET-06-0423), Shuguang Project (06SG28), and Shanghai Leading Academic Discipline Project (B409). This work is supported by the National Natural Science Foundation of China (20590366), the Ministry of Science and Technology of China (2007AA05Z101), and the Science and Technology Commission of Shanghai Municipality (05DJ14002).

Literature Cited

1. Hudlicky M. *Oxidation in Organic Chemistry*. Washington, DC: American Chemical Society, 1990.
2. Sheldon RA, Kochi JK. *Metal-Catalyzed Oxidations of Organic Compounds*. New York: Academic Press, 1981.
3. Mallat T, Baiker A. Oxidation of alcohols with molecular oxygen on solid catalysts. *Chem Rev*. 2004;104:3037–3058.
4. Cainelli G, Cardillo G. *Chromium Oxidants in Organic Chemistry*. Berlin: Springer, 1984.
5. Su FZ, Cao Y. Ga-Al mixed-oxide-supported gold nanoparticles with enhanced activity for aerobic alcohol oxidation. *Angew Chem Int Ed*. 2008;47:334–337.
6. Sheldon RA, Arends IWCE, Brink GJT, Dijksman A. Green, catalytic oxidations of alcohols. *Acc Chem Res*. 2002;35:774–781.
7. Deshpande SS, Jayaram RV. A facile deprotection of oximes over mixed metal oxides under solvent-free conditions. *Catal Commun*. 2008;9:639–644.
8. Shen J, Shan W, Zhang Y, Du J, Xu H, Fan K, Shen W, Tang Y. Gas-phase selective oxidation of alcohols: In situ electrolytic nano-silver/zeolite film/copper grid catalyst. *J Catal*. 2006;237:94–101.
9. Yamamoto R, Sawayama Y, Shibahara H, Ichihashi Y, Nishiyama S, Tsuruya S. Promoted partial oxidation activity of supported Ag catalysts in the gas-phase catalytic oxidation of benzyl alcohol. *J Catal*. 2005;234:308–317.
10. Mao JP, Deng MM, Xue QS, Chen L, Lu Y. Thin-sheet Ag/Ni-fiber catalyst for gas-phase selective oxidation of benzyl alcohol with molecular oxygen. *Catal Commun*. 2009;10:1376–1379.
11. Pestryakov AN, Lunin VV, Bogdanchikova NE, Petranovskii VP, Knop-Gericke A. Supported foam-silver catalysts for alcohol partial oxidation. *Catal Commun*. 2003;4:327–331.
12. Pestryakov AN, Bogdanchikova NE, Knop-Gericke A. Alcohol selective oxidation over modified foam-silver catalysts. *Catal Today*. 2004;91:49–52.
13. Magaev OV, Knyazev AS, Vodyankina OV, Dorofeeva NV, Salanov AN, Boronlin AI. Active surface formation and catalytic activity of phosphorus-promoted electrolytic silver in the selective oxidation of ethylene glycol to glyoxal. *Appl Catal A*. 2008;344:142–149.
14. Pina CD, Falletta E, Rossi M. Highly selective oxidation of benzyl alcohol to benzaldehyde catalyzed by bimetallic gold-copper catalyst. *J Catal*. 2008;260:384–386.
15. Chang BK, Lu Y, Tatarchuk BJ. Microfibrous entrapment of small catalyst or sorbent particulates for high contacting-efficiency

removal of trace contaminants including CO and H_2S from practicle reformates for PEM H_2-O_2 fuel cells. *Chem Eng J*. 2006;115:195–202.
16. Lu Y, Sathitsukasnoh N, Queen A, Tatarchuk BJ. Microfibrous entrapped ZnO/support sorbents for high contacting efficiency H_2S removal from reformate streams in PEMFC Applications. In: Wang Y, Holladay JD, editors. *Microreactor Technology and Process Intensification*. New York, NY: American Chemical Society Publications Division, Distributed by Oxford University Press, 2005.
17. Lu Y, Wang H, Liu Y, Xue QS, Chen L, He MY. Novel microfibrous composite bed reactor: high efficiency H_2 production from NH_3 with potential for portable fuel cell power supplies. *Lab Chip*. 2007;7:133–140.
18. Liu Y, Wang H, Li JF, Lu Y, Xue QS, Chen L. Microfibrous entrapped Ni/Al_2O_3 using SS-316 fibers for H_2 production from NH_3. *AIChE J*. 2007;53:1845–1849.
19. Wang MM, Li JF, Chen L, Lu Y. Miniature NH_3 cracker based on microfibrous entrapped $Ni\text{-}CeO_2/Al_2O_3$ catalyst monolith for portable fuel cell power supplies. *Intl J Hydrogen Energy*. 2009;34:1710–1716.
20. Liu Y, Wang H, Li JF, Lu Y, Wu HH, Xue QS, Chen L. Monolithic microfibrous nickel catalyst co-modified with ceria and alumina for miniature hydrogen production via ammonia decomposition. *Appl Catal A*. 2007;328:77–82.
21. Harris DK, Cahela DR, Tatarchuk BJ. Wet layup and sintering of metal-containing microfibrous composites for chemical processing opportunities. *Compos A: Appl Sci Manuf*. 2001;32: 1117–1126.
22. Gavriilidis A, Sinno B, Varma A. Influence of loading on metal surface area for $Ag/\alpha\text{-}Al_2O_3$ catalysts. *J Catal*. 1993;139:41–47.
23. Pestryakov AN. Modification of silver catalysts for oxidation of methanol to formaldehyde. *Catal Today*. 1996;28:239–244.
24. Pestryakov AN, Davydov AA. Active electronic states of silver catalysts for methanol selective oxidation. *Appl Catal A*. 1994;120:7–15.
25. Waterhouse GIN, Bowmaker GA, Metson JB. Oxygen chemisorptions on an electrolytic silver catalyst: a combined TPD and Raman spectroscopic study. *Appl Surf Sci*. 2003;214:36–51.
26. Waterhouse GIN, Bowmaker GA, Metson JB. Mechanism and active sites for the partial oxidation of methanol to formaldehyde over an electrolytic silver catalyst. *Appl Catal A*. 2004;265:85–101.
27. Rhodes HE, Wang P-K, Stokes HT, Slichter CP, Sinfelt JH. NMR of platinum catalysts. I. Line shapes. *Phys Rev B*. 1982;26:3559–3568.
28. Yu I, Gibson AA, Hunt RE, Halperin WP. Observation of conduction-electron density oscillations at the surface of platinum particles. *Phys Rev Lett*. 1980;44:348–351.
29. Stokes HT, Rhodes HE, Wang P-K, Slichter CP, Sinfelt JH. NMR of platinum catalysts. III. Microscopic variation of the Knight shifts. *Phys Rev B*. 1982;26:3575–3581.
30. Jing F, Tong H, Kong L, Wang C. Electroless gold deposition on silicon(100) wafer based on a seed layer of silver. *Appl Phys A*. 2005;80:597–600.
31. Ye W-C, Ma C-L, Shang W, Chen Y, Wang R, Wang C-M. Effect of sodium dodecylsulfate on improving microstructural properties of electroplated silver-oxygen-tungsten thin films. *Surf Coat Tech*. 2007;201:9456–9461.
32. Wagner CD, Zatko DA, Raymond RH. Use of the oxygen KLL Auger lines in identification of surface chemical states by electron spectroscopy for chemical analysis. *Anal Chem*. 1980;52: 1445–1451.
33. Salvati L, Makovsky LE, Stencel JM, Brown FR, Hercules DM. Surface spectroscopic study of tungsten-alumina catalysts using x-ray photoelectron, ion scattering, and Raman spectroscopies. *J Phys Chem*. 1981;85:3700–3707.
34. Kumar KV. XPS core level spectra and Auger parameters for some silver compounds. *J Electron Spectrosc Relat Phemon*. 1991;56: 273–277.
35. Brion D. Photoelectron spectroscopic study of the surface degradation of pyrite (FeS_2), chalcopyrite ($CuFeS_2$), sphalerite (ZnS), and galena (PbS) in air and water. *Appl Surf Sci*. 1980;5:133–152.
36. Tsutsumi T, Ikemoto I, Namikawa T, Kuroda H. X-ray photoelectron spectrum of chromium oxide (Cr_2O_5). *Bull Chem Soc Jpn*. 1981;54:913–914.

Manuscript received May 8, 2009, and revision received Sept. 2, 2009.